TÜBİTAK

Turkish Journal of Earth Sciences

http://journals.tubitak.gov.tr/earth/

Research Article

Turkish J Earth Sci
(2016) 25: 289-299

doi:10.3906/yer-1509-6

The depth effect of earthquakes on tsunami heights in the Sea of Okhotsk

Andrey ZAYTSEV[1,2], Irina KOSTENKO[1,2], Andrey KURKIN[2], Efim PELINOVSKY[1,2,3], Ahmet Cevdet YALÇINER[4,*]

[1]Laboratory of Computational Hydrophysics and Oceanography, Special Research Bureau for Automation of Marine Researches. Yuzhno-Sakhalinsk, Russia

[2]Laboratory for Hazard Prediction, Nizhny Novgorod State Technical University n.a. P.E. Alekseev, Nizhny Novgorod, Russia

[3]Department of Nonlinear Geophysical Processes, Institute of Applied Physics, Nizhny Novgorod, Russia

[4]Department of Civil Engineering, Ocean Engineering Research Center, Middle East Technical University, Ankara, Turkey

Received: 09.09.2015 • **Accepted/Published Online:** 08.03.2016 • **Final Version:** 09.06.2016

Abstract: The earthquake of magnitude M_w = 8.3 that occurred on 24 May 2013 in the Sea of Okhotsk was the most powerful earthquake in the region. Fortunately, the generated tsunami was small because of the deep focal depth (609 km) and was only detected by the nearest Deep-ocean Assessment and Reporting of Tsunamis (DART) buoy records. However, the event highlighted the fact that any earthquakes with similar magnitudes at shallower focal depths would have caused considerable tsunamis. In order to evaluate the effects of possible tsunamis in the Sea of Okhotsk, we simulated water displacements due to the 24 May 2013 event and compared the results with the measurements. Moreover, the simulations were extended using different shallower focal depths. In simulations we calculated the coastal amplifications and possible heights of the tsunami waves along the coast of the Sea of Okhotsk.

Key words: Earthquake, tsunami, numerical modeling, simulation, amplification, Sea of Okhotsk

1. Introduction

On 24 May 2013 at 05:44:49 UTC a strong earthquake occurred in the western part of the Sea of Okhotsk. According to the Geological Survey of the Russian Academy of Sciences (GSRAS, 2016), the magnitude of the main shock was 8.3 and the epicenter coordinates were 54.874°N, 153.281°E with a focal depth of 609 km (Figure 1). The other characteristics of the earthquake were presented by Ye et al. (2013). The Sakhalin Tsunami Center declared a tsunami warning for the entire coast of the Sakhalin and Kuril Islands in the Sea of Okhotsk. The warning was cancelled on 24 May at 06:17 hours, 33 min after the earthquake. It should be noted that this was the strongest earthquake known in the history of the Sea of Okhotsk region (USGS, 2016). Seismic waves produced by this earthquake spread over long distances and led to tremors at a distance of up to 8000 km; they were felt in the central part of Russia, including Moscow and Nizhny Novgorod (Tatevossian et al., 2014). However, the focal depth of 609 km with even a such a large magnitude (M = 8.3) is too deep to cause noticeable tsunami waves. Had the focal depth been less, the tsunami waves could have been noticeable and even catastrophic. Seismotectonic properties of the Sea of Okhotsk were described by Tikhonov and Lomtev (2015). They analyzed shallow earthquakes with focal depths of less than 60 km and identified the peripheral character of shallow earthquakes in the Sea of Okhotsk. Such earthquakes induced tsunamis in the past. For assessment of tsunami hazard it is necessary to analyze all possible tsunami source locations, and this will be done in the future. Here we will consider only one earthquake of 2013 for study of the depth effect. Taking into account the relative small size of the Sea of Okhotsk we may expect that some results will be valid for other earthquakes locations in the Sea of Okhotsk. It should also be noted that the parameters of the earthquakes may change due to the types of subductions (i.e. Chilean type subduction, Mariana type subduction). The dip of the subduction is important and may differ between different subduction zones. For example, the dip of the Chilean subduction is lower than the Mariana subduction, which may cause larger earthquakes in the Chilean type than the Mariana type. The dip of the earthquakes also changes in various depths of the subduction (Uyeda and Kanamori, 1979).

The main objectives of this study are to evaluate the tsunami rupture parameters by simulation and comparison with the Deep-ocean Assessment and Reporting of Tsunamis (DART) records and to evaluate the possible coastal amplification of tsunami waves that could have

* Correspondence: yalciner@metu.edu.tr

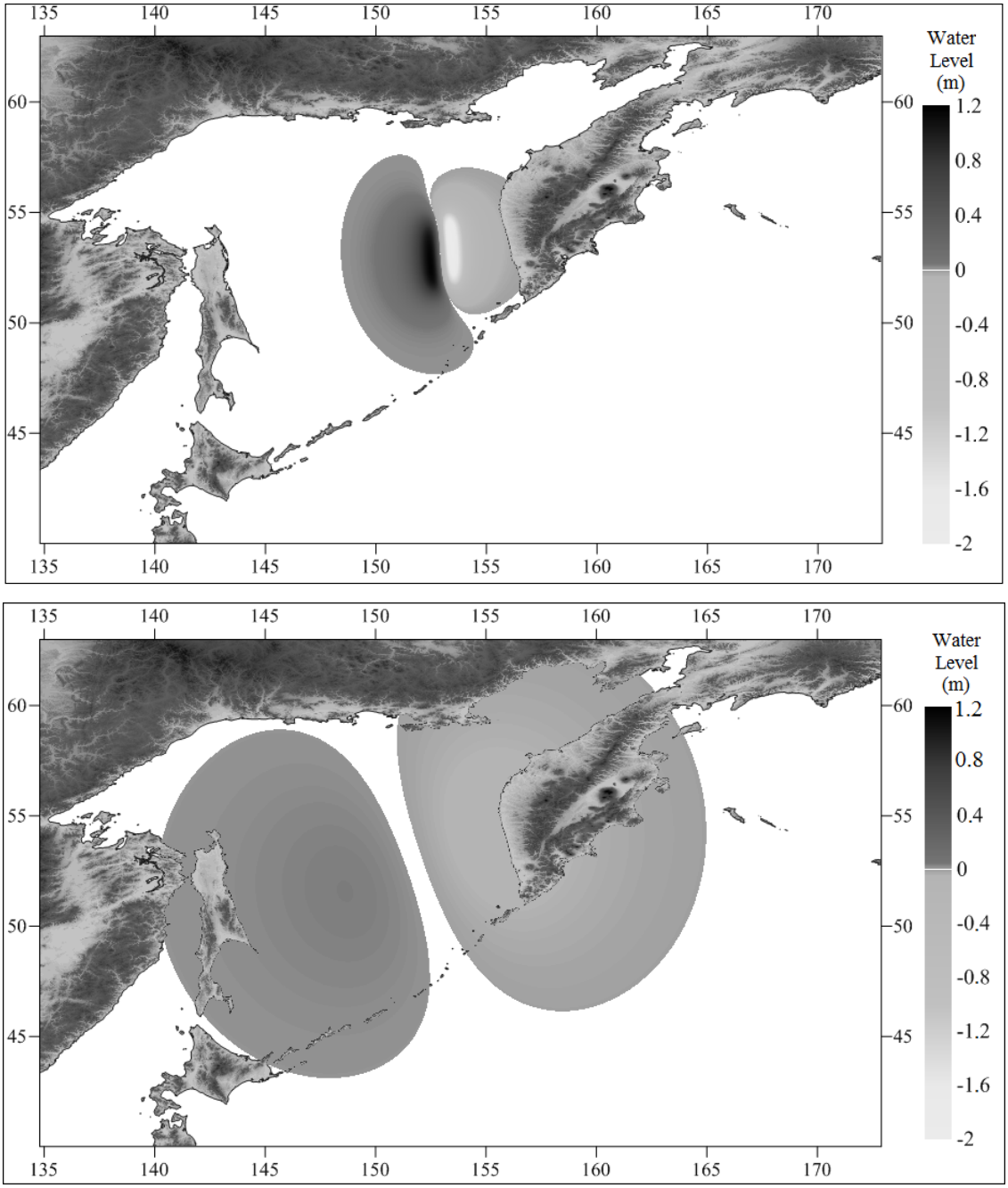

Figure 1. The initial displacement of the sea surface at the tsunami source due to different focal depths: a) focal depth of 60 km; b) focal depth of 609 km.

occurred with the tsunami related to the earthquake parameters of 24 May 2013 in the case of shallower focal depths. The tsunami source is computed by using the tsunami simulation and visualization code NAMI DANCE (NAMI DANCE, 2016) by using the static vertical deformation algorithm developed by Okada (1985) and Manshinha and Smylie (1971). The calculations confirm the well-known fact that a powerful earthquake with a focal depth of less than 100 km could cause a destructive tsunami in the region. Nevertheless, the unexpected result of the calculations was that even in the case of a deep-focused earthquake, the displacement of the water level at the epicenter might be in several centimeters, and therefore could easily be recorded by modern instruments such as DART buoys.

2. The tsunami source

The 24 May 2013 earthquake parameters were taken from the Geological Survey of the Russian Academy of Sciences (GSRAS, 2016). The length of the tectonic fault was 300 km, width of the fault was 60 km, strike angle was 177°, dip angle was 10°, rake (slip angle) was –107°, and average slip was 10 m. In the simulations, the focal depth was selected in the range between 609 km and 60 km while the other parameters were kept as they were. Two different tsunami sources calculated by the vertical dislocation algorithm developed by Okada (1985) using 609 km and 60 km focal depths are shown in Figure 1. The subsidence is observed at the east and uplift is observed at the west. The positive and negative amplitudes of the tsunami sources are about 10 times larger when the focal depth is 10 times shallower. Moreover, the size of the tsunami source becomes larger for the shallower focal depth. As anticipated, the size of the seismic area and the average slip in the source are governed by the focal depth (Aki, 1966; Kanamori and Anderson, 1979; Hebert et al., 2001, 2005; Ulutaş et al., 2012; Baptista et al., 2013; Mathias et al., 2013; Ulutaş, 2013). In the case of the shallow-focus earthquake (60 km), the height (the difference between the maximum bottom uplift and its maximum bottom subsidence) is 3.1 m, while in the deep-focus earthquake (609 km) the difference is 0.1 m (Table 1). The last figure turned out to be a surprise, because it meant that a tsunami even with such a large depth of the epicenter can actually be detected by modern means. Generally speaking, Okada's solution describes a static (near) field in the theory of elastic half-space, which rather slowly decreases with distance according to power law. Thus, Okada (1995) in another paper demonstrated a relationship between average slip in the seismic area and the parameters of the point source of an earthquake:

$$\lg H\,[\mathrm{cm}] = 1.5\,M_w - 2\lg h\,[\mathrm{km}] - 5.96, \quad (1)$$

where M_w is earthquake magnitude, H is the maximum height of the bottom of the bias in the seismic area, and h is focal depth. From Eq. (1) it follows that the height decreases inversely proportional to the square of the focal depth. Calculated according to Eq. (1), the maximum displacements in the seismic area are also given in Table 1 (the last column). As can be seen, at the depth of the seismic area of 200 km or more, calculations according to the two different formulas of Okada agree rather well. For shallow-focus earthquakes the approach of point area does not work, as noted by Bolshakova and Nosov (2011).

By the calculations according to Okada's "exact" formula, as well as his approximate formula, the slip of the sea bottom (and hence the water level) in the area of the 2013 Sea of Okhotsk tsunami source might achieve nearly 10 cm (the upward slip about 4 cm, the downward slip about 7 cm). The calculation of the tsunami source naturally depends on the generation model and may vary due to input parameters. Okal (private report) used the source model PREM (Preliminary Reference Earth Model) and obtained the following estimates: the bottom can be raised by 1.3 cm and can be lowered by 2.5 cm, and these estimates were indirectly confirmed by GPS (Okal et al., 2014). Similar calculations were performed for the approximation of the tsunami source according to the formulas of Manshinha and Smylie (1971). In this case, the maximum uplift of the bottom (1.1 cm) occurs at the point with coordinates 55.2°N, 147.2°E and the subsidence (2.2 cm) occurs at 54.0°N, 157.2°E. These points are on the ground of the Kamchatka Peninsula. The value of the slip is also influenced by the value of the Poisson ratio (the combination of Lamé coefficients; for details see Bolshakova and Nosov, 2011), and the latter for the calculations was chosen as 0.25. In any case, it is confirmed that the bottom displacements and the water level of several centimeters should have occurred around the epicenter of the 2013 Sea of Okhotsk earthquake.

3. Data recorded by DART buoys

We analyzed the records of DART buoys closest to the earthquake source. The sampling interval of the records was 15 min; when receiving data on horizontal movements in the water column DART increases sampling to 1 min, while in vertical slip of the water surface over 0.03 m DART switches to intervals of 15 s.

Further on we will present 1-min recordings of the sea level during 5 h on the background of tidal oscillations, which started 45 min before the main shock of the

Table 1. The calculated displacement of the water surface in the seismic area of the tsunami at various depths of focus of the earthquake.

Focus depth, km	Minimum value, m	Maximum value, m	Height, m	Calculation by Eq. (1), m
60	–1.95	1.18	3.13	8.3
100	–1.26	0.75	2.01	3
200	–0.54	0.31	0.85	0.8
400	–0.17	0.1	0.27	0.2
609	–0.07	0.04	0.11	0.07

earthquake. The positions of these buoys are shown in Figure 2. One of them, DART 21419, is located at 44.455°N, 155.736°E. From the recording (Figure 3a) we present the fluctuations of bottom pressure recalculated to the sea level according to the hydrostatic equation. Noticeable fluctuations in the range of tsunami waves (spikes in the recording were removed) began with the 50th minute (5 min after the beginning of the earthquake) and ended approximately at the 125th minute (80 min after the earthquake). The bow wave changes sign: the impulse of positive polarity is followed by the impulse of negative polarity. The maximum height of water level displacement reaches 0.03 m (in the analysis of records with discreteness of 15 s, the wave height increases to 0.09 m). The next noticeable wave of negative polarity up to 0.03 m appears after about 12 min.

Similar oscillations are visible from the recording of Russian DART buoy 21402, located at 46.488°N, 158.343°E (east of the island of Simushir; see Figure 2), and this record is reproduced in Figure 3b. The maximum height of the water level displacement reaches 0.03 m (in the analysis of records with increments of 15 s the wave height increases to 0.18 m).

We also present a record of sea-level fluctuations from DART buoy 21415 (depth 4707 m), located at 50.183°N, 171.847°E (Figure 2), and the record is shown in Figure 3b. The maximum height of the water level's displacement in the analysis of the 1-min recording reaches 0.04 m, and in the analysis of records with increments of 15 s the wave height increases to 0.42 m.

The time entry of submitted waves at all DART buoys is the same, which is impossible in the case of tsunami propagation in the waters of the ocean. As will be shown below, the DART buoys did not record the tsunami waves (or, to be more precise, they were not selected from the background noise), and their oscillations are related to the seismoacoustic processes in the earthquake area. Mathematical models have been developed to describe coseismic acoustic oscillations and tsunami waves simultaneously (Levin and Nosov, 2009; Okal et al., 2014). These models are rather complicated and are not used in this study. We focus only on the calculation of tsunami waves.

4. Simulation of tsunami propagation in the near field

The tsunami source is calculated according to Okada (1985) (Figure 1). The simulations are performed by using the tsunami numerical model NAMI DANCE (NAMI DANCE, 2016). The grid size of the bathymetry used was 0.0075 degrees, which is equivalent to 500–678 m in these latitudes. The duration of tsunami propagation in the Sea of Okhotsk is about 2–3 h; therefore, the numerical simulation was set to 6 h to compute the possible reflection and focusing of energy in the study domain. The reflecting boundary conditions (the approach of the vertical wall) is used on the shore.

First of all, we tried to compare the computed time histories of the water surface at DART locations with the data recorded by DART. This comparison for DART buoy 21419 (depth 5235 m) is shown in Figure 4a. We also used the record of measurements comprising measurement

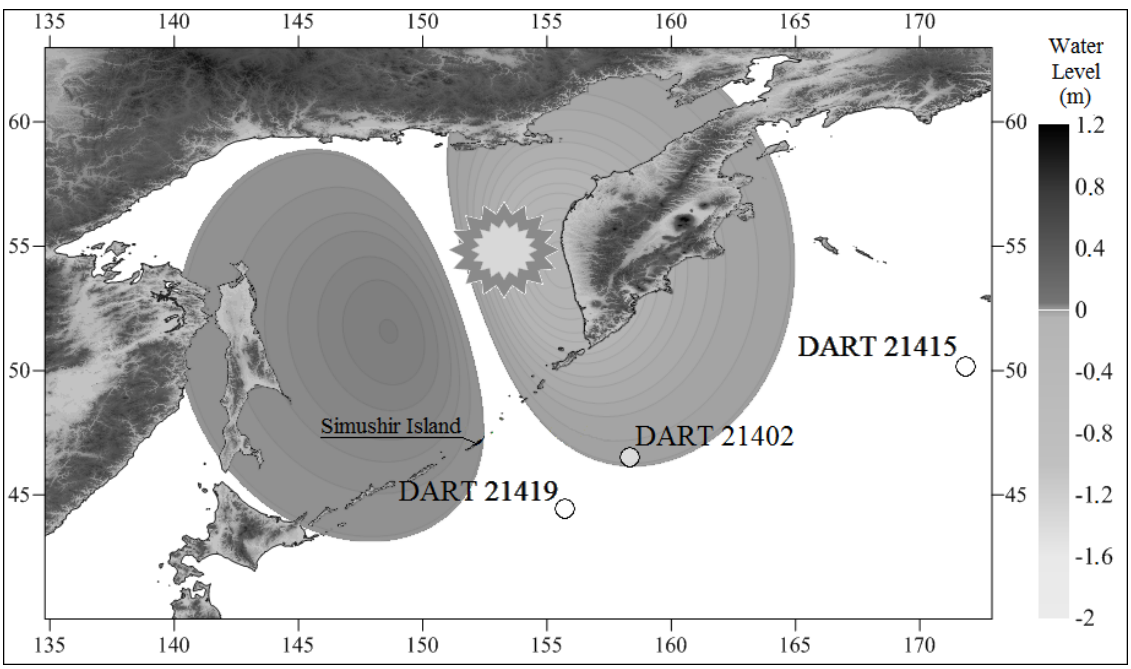

Figure 2. The locations of DART buoys and the epicenter of the 24 May 2013 earthquake.

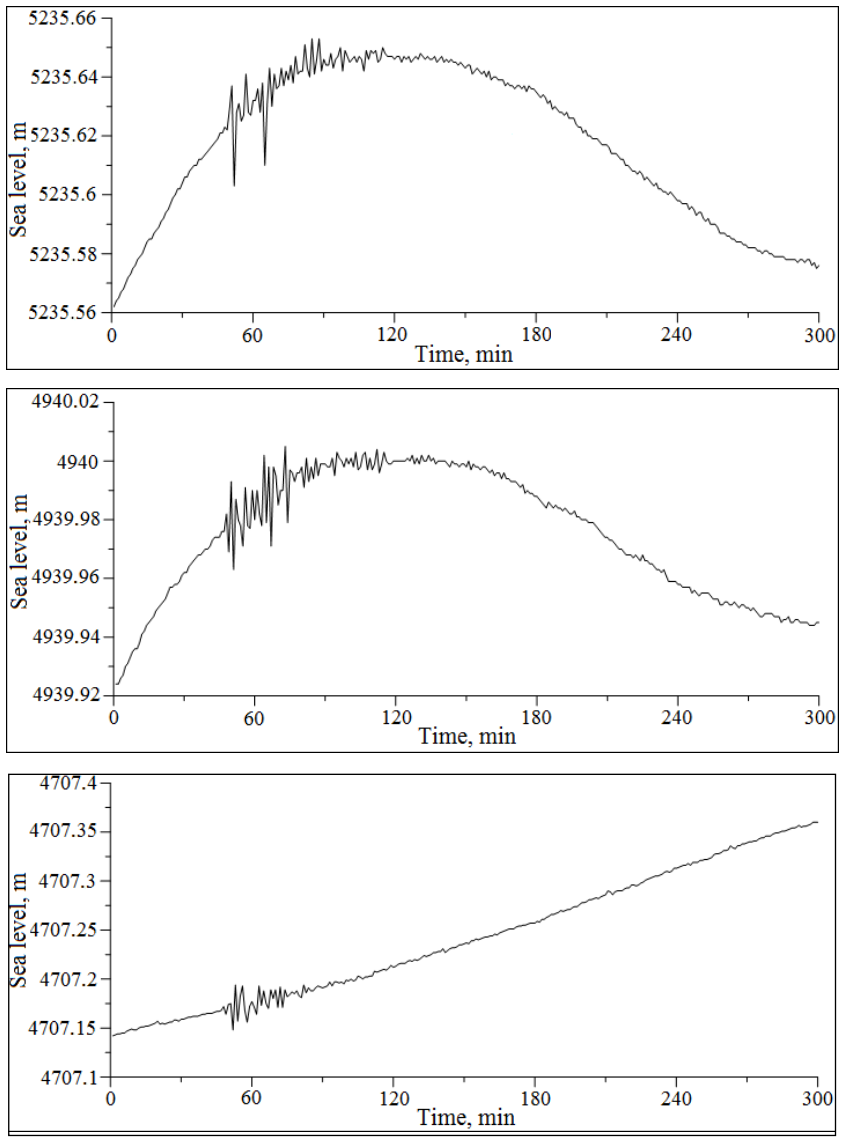

Figure 3. The record of sea-level fluctuations: a) by DART buoy 21419, located at the depth of 5235 m; b) by Russian DART buoy 21402, located at the depth of 4940 m; c) at DART buoy 21415, located at the depth of 4707 m (the vertical axis is the elevation of water level from the ocean bottom and the horizontal axis the time in hours and starts from 24 May 2015 at 05:00 UTC (44 min and 49 s before the earthquake)).

samplings of 1 min and 15 s, and the observed record was cleared of tidal oscillations. It is clearly seen that the initial relatively large (0.09 m) water-level fluctuations recorded for the buoy were not related to the tsunami waves that developed later (after about 20 min). The reason for the preliminary fluctuations in the record is seismoacoustic phenomena during the earthquake. They mask weak tsunamis in the seismic area. In fact, the calculations first show a lowering of the sea level to the height of about 0.01 m for 1 h and then a rise to 0.02 m for 1 h. Against this background a weak noise signal at the limit of computing accuracy was noticeable.

Similar results are obtained for DART buoy 21402, depth 4940 m (Figure 4b). DART recorded short fluctuations of about 20 cm at the time of the earthquake. The calculations show the evolution of residual displacement, as well as the appearance of a small wave of negative polarity with an amplitude of about 0.04 m; this wave occurred immediately after the main shock. A rise of the water level of 0.01 m occurred 1 h later.

DART buoy 21415 demonstrates the greatest shift in the seismic area (0.42 m), as can be seen in Figure 4b. The calculations show the appearance of low-frequency lowering of the water level (0.04 m), which lasted nearly

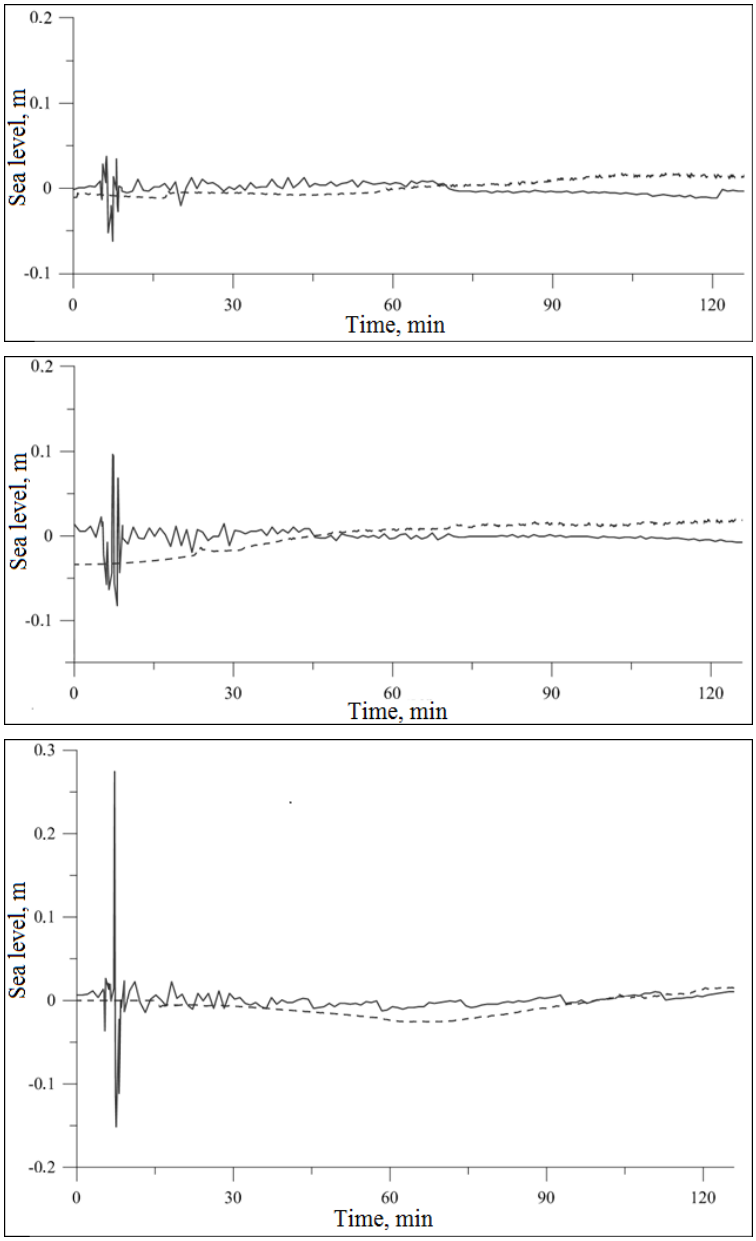

Figure 4. The comparison of the computed and measured results of the sea level: a) at DART 21419 (depth 5235 m); b) at DART 21402 (depth 4940 m); c) at DART 21415 (depth 4707 m) (solid line: measured, dashed line: computed).

1 h, as well as a weak tsunami wave with an amplitude of about 0.01 m at 120 min after the earthquake.

The above comparison shows the difficulties of using DART buoys at the tsunami source to detect weak tsunami waves masked by seismoactive processes.

5. Simulation of tsunami propagation in the far field

The propagation of a tsunami in the far field was studied using different focal depths in different simulations by keeping the other rupture parameters the same. Figure 5 shows the sea state at 1 h and 2 h after the earthquake in the case of a shallow-focused earthquake with focal depth of 60 km. One hour later the tsunami waves propagated in almost the entire area of the Sea of Okhotsk as well as the part of the Pacific Ocean adjacent to the Kuril Islands. Two hours later the tsunami waves began to penetrate the shallow areas of the Sea of Okhotsk with a significantly reduced speed (due to shallow water depths) and to transmit from the Kuril Isles to the Pacific Ocean. The maximum wave heights in the calculation area are presented in Tables 2–4. These maximum values were obtained for waves in the shallow area, so they grew with time as the wave penetrated deeper

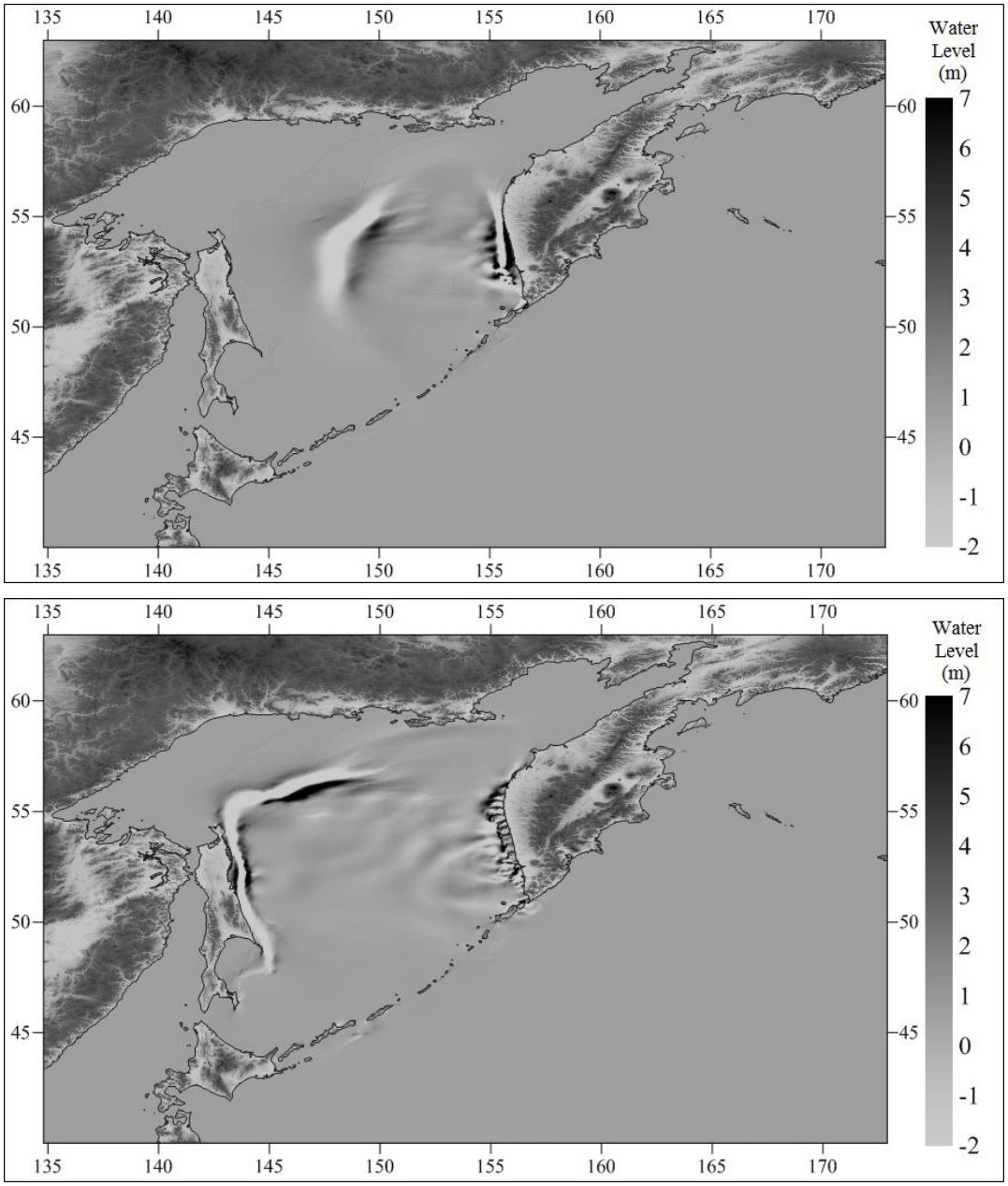

Figure 5. The sea state at 1 h (a) and 2 h (b) after the earthquake (in the case of 60 km focal depth).

Table 2. The calculated wave heights after 1 h at various focal depths.

Focus depth, km	Minimum value, m	Maximum value, m
60	–2.19	1.83
100	–1.29	1.06
200	–0.66	0.35
400	–0.26	0.19
609	–0.11	0.09

Table 3. The calculated wave height after 2 h at different focal depths.

Focus depth, km	Minimum value, m	Maximum value, m
60	–1.55	8.72
100	–1.03	3.54
200	–0.31	1.97
400	–0.21	0.50
609	–0.12	0.3

Table 4. The distribution of the maximum amplitudes of tsunami waves in the Sea of Okhotsk.

Focal depth, km	Maximum value of the positive amplitude, m
60	8.8
100	4.02
200	2.08
400	0.75
609	0.3

into the shallow water, where it was amplified. In the case of the shallow earthquake (60 km), the maximum wave heights achieved catastrophic values of 4–6 m, becoming very dangerous. However, even if the focal depth was 100 km, the wave heights would have amplified to 2–4 m. Therefore, such a tsunami would have also been disastrous. With the actual focal depth of the earthquake (609 km), the maximum wave heights, according to the calculations, were about 30 cm. Therefore, the tsunami waves could not be observed clearly.

The effect of the focal depth on the calculated characteristics of the tsunami is also presented in Figure 6, given on logarithmic and semilogarithmic scales. These scales show that 1 h later the calculation data are well approximated by a power law with a slope of 1.24:

$$\ln A\ [\text{cm}] = 5.72 - 1.24 \ln h\ [\text{km}], \quad (2)$$

where A is the so-called maximal positive amplitude of the wave calculated in the whole domain. On large time scales, the calculated maximum amplitude of the wave depends on the depth exponentially. Thus, for the whole time of the calculations, this dependence is approximated by the following formula:

$$\ln A\ [\text{cm}] = 1.79 - 0.005\, h\ [\text{km}]. \quad (3)$$

The distribution of the maximum values of the tsunami wave's positive amplitudes in the Sea of Okhotsk with a small focal depth (60 km) in the simulation duration is shown in Figure 7. It shows that the direction of the main energy of the tsunami is towards the west coast of the Kamchatka Peninsula and the northeastern coast of Sakhalin.

It is also important to evaluate and discuss the areas of the maximum impact of a tsunami with a shallow focal-depth (60 km) earthquake with similar rupture parameters. According to the simulation results, the northeastern part of Sakhalin Island (Figure 8a) was mostly affected. In fact, on the entire eastern coast of Sakhalin, the nearshore water elevation exceeds 1.5 m. In the case of the actual focal depth (609 km) the wave height at the source is 0.2 m. The distributions of the maximum water elevations computed along the east coast of Sakhalin Island according to the simulations with two different focal depths are shown in Figure 8a. It is seen that the distributions are different and

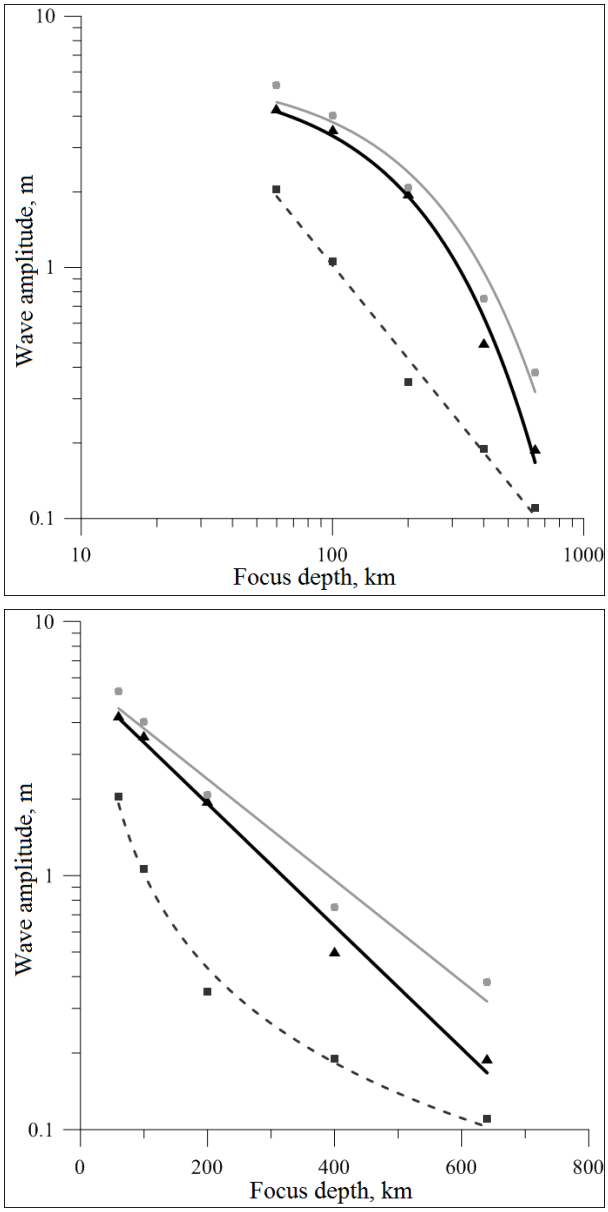

Figure 6. The computed tsunami amplitudes with respect to the focal depth (■ - 1 h later, ▲ - 2 h later, and ● - for the entire time of calculations). The lines are the corresponding regression lines.

the average of the maximum water elevations along the east of Sakhalin is about 15 times higher when focal depth is reduced to be about 10 times more shallow (from 609 km to 60 km).

The distributions of the maximum nearshore water elevations computed along the west coast of the Kamchatka Peninsula for the two different focal depths are also shown in Figure 8b. The computed maximum nearshore water elevations along the west coast of the Kamchatka Peninsula are located between 52°N and 55°N. The maximum values (5.4 m) in the simulation with focal depth of 60 km can

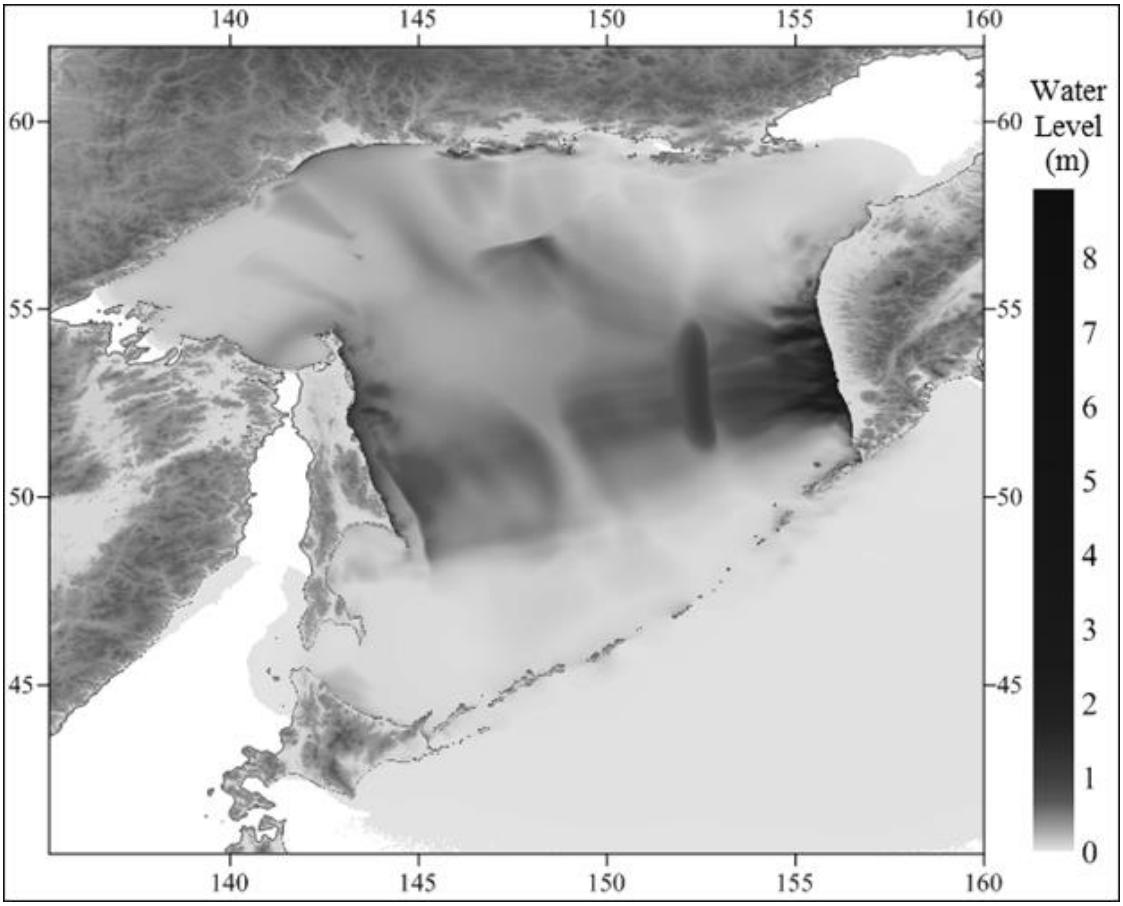

Figure 7. The distribution of the computed maximum water elevations in the Sea of Okhotsk throughout the simulations using the focal depth of 60 km.

be observed to the north of Oktyabrskiy settlement. When being modeled with the focal depth of 609 km, the maximum nearshore water elevations become 0.45 m; they can be obtained in the area a short distance to the south, near the settlement of Bolsheretsk.

The average of maximum nearshore wave amplitudes on the east coast of Sakhalin Island (Figure 8a) and on the west coast of Kamchatka Peninsula (Figure 8b) are also computed and tabulated in Table 5. It is seen from the table that when focal depth decreases 10 times, from 609 km to 60 km, the average of maximum nearshore positive amplitudes on west coast of Kamchatka and east coast of Sakhalin will increase about 15 times.

Table 5. The average amplitudes of tsunami waves on the Sakhalin and Kamchatka coasts due to focal depths of 60 km and 609 km.

Location	Focal depth, km	Average value of the positive amplitude, m
Sakhalin	609	0.09
Sakhalin	60	1.43
Kamchatka	609	0.15
Kamchatka	60	2.87

6. Conclusion

The strongest earthquake of 24 May 2013 in the Sea of Okhotsk did not cause a significant tsunami due to the deep focal depth (609 km), though it was recorded by DART buoys. Parameters of the tsunami source were chosen according to Okada's solution. These parameters are close to the calculations by Professor Okal from other models Okal (2015, personal communication). In the worst case, the estimated height of the tsunami waves off the coast of Sakhalin and Kamchatka could reach 20–40 cm and, in fact, could be observed by equipment if it were installed in the Sea of Okhotsk. The indirect relation between the nearshore tsunami amplitude and focal depth shows that nearshore amplitude increases exponentially with decreasing focal depth. In the case of deep submarine earthquakes (609 km focal depth) the tsunami waves

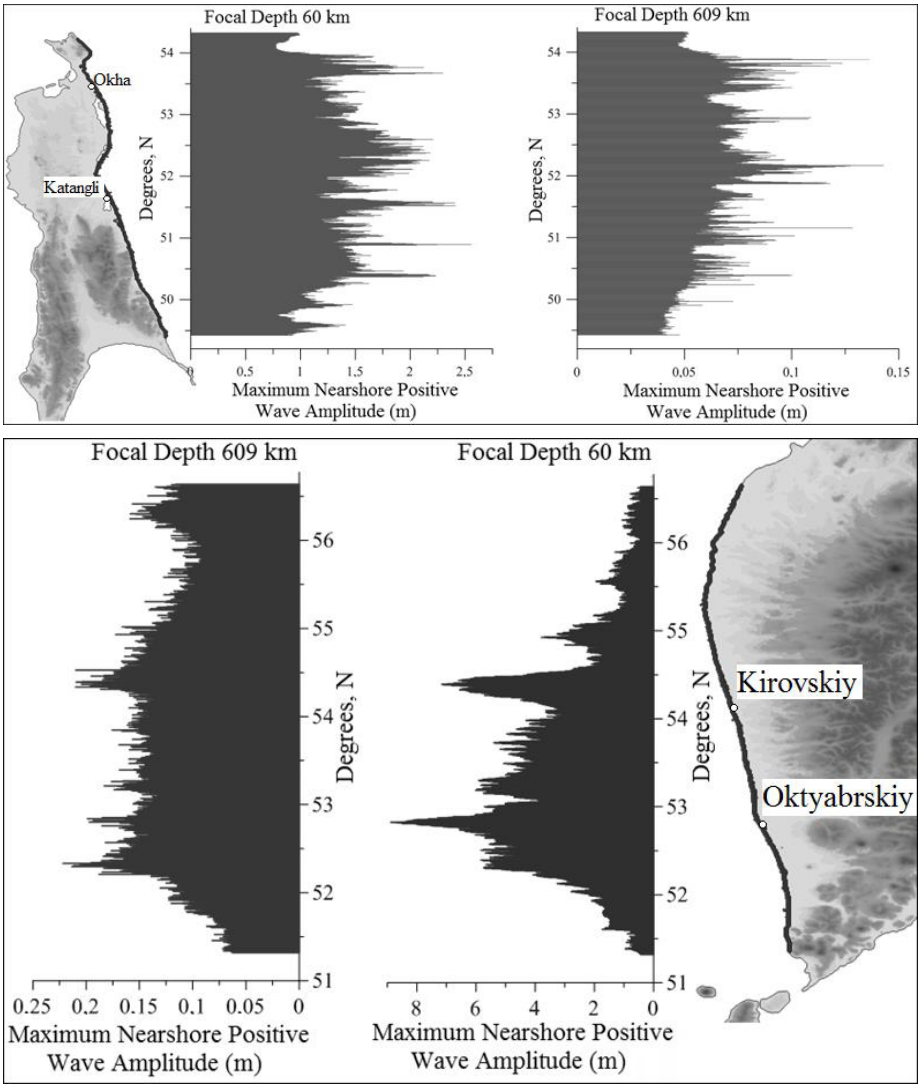

Figure 8. The distribution of the computed maximum nearshore positive wave amplitudes along the eastern coast of Sakhalin (a) and western coast of the Kamchatka Peninsula (b).

cannot be observed clearly in the Sea of Okhotsk. If the focal depth had been shallow, for example 60 km, the tsunami would have been effective and the wave height would have reached several meters, mainly along the east of Sakhalin Island and the west of the Kamchatka Peninsula. The analysis of the 2013 Sea of Okhotsk tsunami event given in this study, along with previous studies (Kim and Rabinovich, 1990; Lobkovsky et al., 2006, 2009; Zaitsev et al., 2008; Baranov et al., 2013), indicates the importance of a special study on tsunami hazard assessment in the Sea of Okhotsk. The tsunami source was calculated from the elastic dislocation theory using the algorithm of Okada (1985). However, the faults do not rupture with average slip. There are different subfaults that rupture in different displacements, called a finite fault (Lay et. al., 2011; Newman et al., 2011; Romano et al., 2011; Yokota et al., 2011). In further study, a finite fault approach can be utilized when more data are available.

Acknowledgments

The presented results were obtained by partial support of the state task № 2015/133 ("Organization of Scientific Research" and project number 2839), and the work was supported by grants of RFBR (14-05-91370_CT_a, 14-05-00092), MK-4315. 2015.5, and FEB RAS 15-II-1-044 in Russia. The authors thank M Nosov and E Okal for helpful comments. This study was also partly supported by the Scientific and Technological Research Council of Turkey (TÜBİTAK) and the Russian Foundation for Basic Research (RFBR) Joint Research Project Fund, Grant No: TÜBİTAK 213M534, and the ASTARTE Project funded by the European Commission, Grant No. 603839.

References

Aki K (1966). Generation and propagation of G waves from the Niigata earthquake of June 16, 1964. Bull Earthq Res Inst 44: 73-88.

Baranov BV, Lobkovskii LI, Kulikov EA, Rabinovich AB, Jin YK, Dozorova KA (2013). Landslides on the eastern slope of Sakhalin Island as possible tsunami sources. Doklady Earth Sciences 449: 354-357.

Bolshakova AV, Nosov MA (2011). Parameters of tsunami source versus earthquake magnitude. Pure Appl Geophys 168: 2023-2031.

GSRAS (2016). Geological Survey of the Russian Academy of Sciences, Geophysical Survey. Obninsk, Russia: GSRAS. Available online at http://www.ceme.gsras.ru/cgi-bin/ceme/equakes.pl?l=1.

Hebert H, Schindele F, Altinok Y, Alpar B, Gazioglu C (2005). Tsunami hazard in the Marmara Sea (Turkey): a numerical approach to discuss active faulting and impact on the Istanbul coastal areas. Mar Geol 215: 23-43.

Hebert H, Shindele F, Heinrich P (2001). Tsunami risk assessment in the Marquesas Islands (French Polynesia) through numerical modeling of generic far-field events. Nat Hazard Earth Syst 1: 233-242.

Kanamori H, Anderson DL (1975). Theoretical basis of some empirical relations in seismology. Bull Seismol Soc Am 65: 1073-1095.

Kim XS, Rabinovich AB (1990). Tsunamis on the north-west coast of the Okhotsk Sea. In: Natural Catastrophes and Hazards in the Far East Region. Vladivostok, Russia: Far East Branch of the USSR Academy of Sciences Press, pp. 206-218.

Lay T, Ammon CJ, Kanamori H, Yamazaki Y, Cheung KF, Hutko AR (2011). The 25 October 2010 Mentawai tsunami earthquake (Mw 7.8) and the tsunami hazard presented by shallow megathrust ruptures. Geophys Res Lett 38: L06302.

Levin B, Nosov M (2009). Physics of Tsunamis. Doetinchem, the Netherlands: Springer.

Lobkovsky LI, Mazova RKh, Kataeva LYu, Baranov BV (2006). Generation and propagation of catastrophic tsunamis in the Sea of Okhotsk basin: possible scenarios. Doklady Earth Sciences 410: 1156-1159.

Lobkovsky LI, Rabinovich AB, Kulikov EA, Ivashchenko AI, Fine IV, Thomson RE, Ivelskaya TN, Bogdanov GS (2009). The Kuril earthquakes and tsunamis of November 15, 2006, and January 13, 2007: observations, analysis, and numerical modeling. Oceanology 49: 166-181.

Manshinha L, Smylie DE (1971). The displacement fields of inclined faults. Bull Am Seismol Soc 61: 1433-1440.

Matias LM, Cunha T, Annunziato A, Baptista MA, Carrilho F (2013). Tsunamigenic earthquakes in the Gulf of Cadiz: fault model and recurrence. Nat Hazard Earth Syst 13: 1-13.

NAMI DANCE (2016). NAMI DANCE Manual. Ankara, Turkey: METU. Available online at http://namidance.ce.metu.edu.tr/pdf/NAMIDANCE-version-5-9-manual.pdf.

Newman AV, Hayes G, Wei Y, Convers J (2011). The 25 October 2010 Mentawai tsunami earthquake, from real-time discriminants, finite-fault rupture, and tsunami excitation. Geophys Res Lett 38: L05302.

Okada Y (1985). Surface deformation due to shear and tensile faults in a half-space. Bull Seismol Soc Am 75: 1135-1154.

Okada Y (1995). Simulated empirical law of coseismic crustal deformation. J Phys Earth 43: 697-713.

Okal E, Saloor N, Freymueller J, Steblov G, Kogan M (2014). The implosive component of the 2013 Okhotsk Sea deep earthquake: evidence from radial modes and constraints from geodetic data. Geophysical Research Abstracts 16: EGU2014-16456.

Romano F, Piatanesi A, Lorito S, Agostino ND, Hirata K, Atzori S, Yamazaki Y, Cocco M (2012). Clues from joint inversion of tsunami and geodetic data of the 2011 Tohoku–Oki earthquake. Scientific Reports 2: 1-8.

Tatevossian RE, Kosarev GL, Bykova VV, Matsievskii SA, Ulomov IV, Aptekman ZhYa, Vakarchuk RN (2014). A deep-focus earthquake with Mw = 8.3 felt at a distance of 6500 km. Izvestiya Physics Solid Earth 50: 453-461.

Tikhonov IN, Lomtev VL (2015). Shallow seismicity of the Sea of Okhotsk and its probable tectonic nature. Seismic Instruments 51: 111-128.

Ulutaş E (2013). Comparison of the seafloor displacement from uniform and non-uniform slip models on tsunami simulation of the 2011 Tohoku–Oki earthquake. J Asian Earth Sci 62: 568-585.

Ulutaş E, Inan A, Annunziato A (2012). Web-based tsunami early warning system: a case study of the 2010 Kepulaunan Mentawai earthquake and tsunami. Nat Hazard Earth Syst 12: 1855-1871.

USGS (2016). Magnitude 8 and Greater Earthquakes Since 1900. Reston, VA, USA: USGS. Available online at http://earthquake.usgs.gov/earthquakes/eqarchives/year/mag8/magnitude8_1900_date.php.

Uyeda S, Kanamori H (1979). Back-arc opening and the mode of subduction. J Geophys Res 84: 1049-1061.

Ye L, Lay T, Kanamori H, Koper KD (2013). Energy release of the 2013 Mw 8.3 Sea of Okhotsk earthquake and deep slab stress heterogeneity. Science 341: 1380-1384.

Yokota Y, Koketsu K, Fujii Y, Satake K, Sakai S, Shinohara M, Kanazawa T (2011). Joint inversion of strong motion, teleseismic, geodetic, and tsunami datasets for the rupture process of the 2011 Tohoku earthquake. Geophys Res Lett 38: L00G21.

Zaitsev AI, Kovalev DP, Kurkin AA, Levin BW, Pelinovsky EN, Chernov AG, Yalciner A (2008). The Nevelsk tsunami on August 2, 2007: instrumental data and numerical modeling. Doklady Earth Sciences 421: 867-870.